

## Dynamics and trends in excited-state production in collisions of inert gas projectiles with surfaces

This article has been downloaded from IOPscience. Please scroll down to see the full text article.

1995 J. Phys.: Condens. Matter 7 L261

(<http://iopscience.iop.org/0953-8984/7/18/002>)

View [the table of contents for this issue](#), or go to the [journal homepage](#) for more

Download details:

IP Address: 171.66.16.179

The article was downloaded on 13/05/2010 at 13:02

Please note that [terms and conditions apply](#).

## LETTER TO THE EDITOR

# Dynamics and trends in excited-state production in collisions of inert gas projectiles with surfaces

S Lacombe†, V Esaulov†, L Guillemot†, O Grizzi‡, M Maazouz†, N Mandarino§ and Vu Ngoc Tuan†

† Laboratoire des Collisions Atomiques et Moléculaires (Unité associé au CNRS), Université Paris Sud, bâtiment 351, 91405 Orsay, France

‡ Centro Atomico Bariloche, 8400 SC de Bariloche, Argentina

§ Dipartimento di Fisica, Università della Calabria, 87036 Arcavacata di Rende, Cosenza, Italy

Received 8 March 1995

**Abstract.** Results of an investigation of the trends and dynamics of excited state production in collisions of inert gas projectiles on Na, Mg, Al and Si surfaces are presented. Measurements of charge fractions and electron spectra are reported. The efficiency of excited auto-ionizing-state production as a function of energy is determined. These results are compared with known gas-phase collision results. The similar general trends suggest that both in gas-phase collisions and in ion-surface scattering, similar primary excitation mechanisms are operative. However, surface-specific electron capture, loss de-excitation and core rearrangement processes lead to a strong modification in final-state distributions and dominant selective production of the lower-lying excited states occurs.

This letter presents the results of an investigation of the trends and dynamics of excitation processes in collisions of inert gas projectiles on Na, Mg, Al and Si surfaces. The objective of this work is the understanding of outer shell excited-state production in atom-surface collisions. Some of these systems, as well as other metal targets, have been the object of various experimental studies in this laboratory and elsewhere [1–12]. In some previous studies of ion scattering on surfaces, ionization and production of excited states that could not be accounted for in terms of the usual framework of resonant electron capture and loss processes was ascribed to ‘binary’ collisions of the projectile with surface atoms. The excitation processes were then arbitrarily discussed in terms of the molecular orbital (MO) electron promotion model [13], which has been successful in describing outer shell excitation processes in gas-phase collisions. Its use for describing such processes in ion-surface collisions has not, to our knowledge, been justified and no attempt at making a systematic study of systems that have also been studied in gas-phase collisions was made.

Here, we briefly give a synthetic presentation of the first results of such a systematic investigation of the characteristics of the trends in ionization and doubly excited auto-ionizing-state production in the scattering of He, Ne and Ar on the above-mentioned targets. A detailed account and more comprehensive results will be presented subsequently [14–16]. These systems were chosen because gas-phase collisions of Na, Mg and Al ions with He and Ne atoms have been studied [17–22] and these results can thus serve for comparison with surface data. We shall first discuss some measurements of charge fractions and discuss

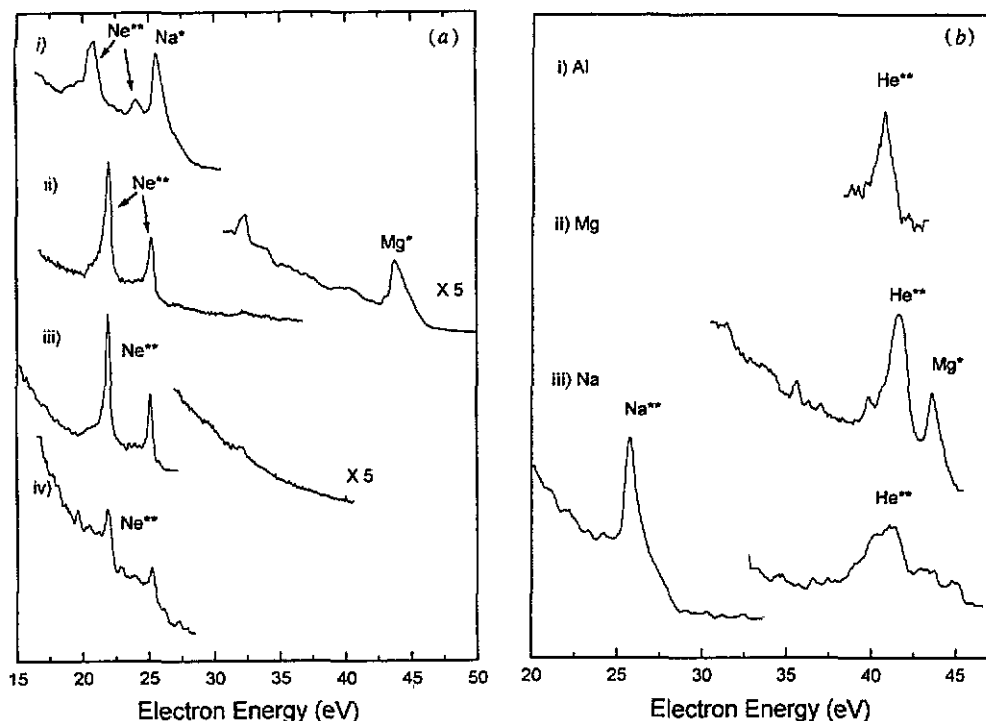


Figure 1. Energy spectra of electrons in the auto-ionizing-state region, produced in (a) 2 keV  $\text{Ne}^+$  collisions incident at  $6^\circ$  on (i) Na,  $90^\circ$  detection, (ii) Mg,  $45^\circ$  detection, (iii) Al,  $45^\circ$  detection and (iv) Si,  $45^\circ$  detection; (b)  $\text{He}^+$  incident at  $6^\circ$  on (i) Al (3 keV ions,  $45^\circ$  detection), (ii) Mg (4 keV ions,  $34^\circ$  detection) and (iii) Na (3 keV ions,  $34^\circ$  detection) targets.

general trends in excited-state production. We then report measurements of the energy dependence of the yield of  $\text{Ne}^{**}$  which are produced in collisions with the targets studied.

Experiments were performed on a UHV set-up described elsewhere [10]. Briefly, electron spectra were acquired using a tandem parallel plate spectrometer, with an energy resolution of 100 meV, for a pass energy of 10 eV. Contrary to what is possible in most systems previously employed for the study of these collisions, measurements could be made for a continuous range of observation angles ( $\alpha$ ) about the incident beam direction, in the  $0$  to  $135^\circ$  range. Ion fractions were determined using a channel electron multiplier fixed behind a second rotatable electrostatic analyser by successively counting neutrals and ions+neutrals. Measurements were performed for ion energies in the 0.5 to 4 keV range, and for incidence angles ( $\phi$ ) in the  $6^\circ$  to  $30^\circ$  range (as measured with respect to the surface plane). Mg, Al and Si samples were mounted vertically on a manipulator which allowed X, Y and Z movements and rotation around the vertical axis. The Mg and Al samples were polycrystalline. The Si single crystal was mounted in an arbitrary orientation and amorphized by prolonged  $\text{Ar}^+$  bombardment. The Na surface was prepared by prolonged evaporation using a Na getter.

We have previously reported ion fraction measurements for  $\text{Ne}^+$  on Mg [10]. A rather large ion fraction was found in agreement with previous studies [6, 7]. Indeed, the ion fraction integrated over scattering angle was found to be of about 14% for 2 keV ions incident at  $6^\circ$  to the surface. It was suggested that this ion fraction is due to binary inelastic collisions with surface atoms, leading to reionization of the Ne atoms formed by neutralization of incident  $\text{Ne}^+$ . In order to confirm this, we now performed measurements

using a *neutral Ne beam* incident on Mg under the same conditions as the  $\text{Ne}^+$  beam. Our measurements show that both the angular distributions of scattered ions and neutrals and the corresponding ion fractions are the same, within the limits of statistical uncertainties. A similar result is observed for Na, Al and Si targets. For both Ne and  $\text{Ne}^+$  scattering on these targets quite large fractions are obtained. Thus for a 2 keV collision energy, the ion fractions integrated over scattering angle were of 35%, 10% and 5% for the Na, Al and Si targets respectively. *The general trend is that for a given energy the charge fractions increase as one goes from Si to Na, i.e. as the collision becomes more 'symmetric'.* One can note already that this is similar to the well known trend in gas-phase collisions where the excitation cross-sections are large for 'symmetric' systems [13].

An indication of the processes that lead to ion production can be obtained from measurements of electron spectra. Typical electron spectra obtained for 2 keV Ne ions incident at  $6^\circ$  to the target surfaces are shown in figure 1. These consists of a continuous distribution on which a series of peaks is superposed. The energy position, and the shape of these structures in the electron spectrum, is dependent on the observation angle and is determined by ejection kinematics, related to emission occurring from a moving source: an excited atom rapidly receding from the surface [10]. This is illustrated on the example of the Na target in figure 2. In the lower-energy part of the spectrum for all targets, there are two main large peaks due to the decay of  $\text{Ne}^{**} 2p^4$  ( $^3\text{P}$  and  $^1\text{D}$ )  $3s^2$  states, whose centre-of-mass energy is close to the 20.35 eV and 23.55 eV positions corresponding to the decay of the excited atom in its free state. At higher electron energies (figure 1(a) i, ii) one generally observes a series of much smaller structures, the largest of which lies close to 30 eV. These are attributable to higher-lying auto-ionizing states of Ne and  $\text{Ne}^+$  [11, 12, 13] with a  $2p^3nln'l'$  configuration. At higher electron energies, for Mg, Al and Si one usually observes structures due to target excitation. Thus in the case of the Mg target (figure 1(a) ii), the structures lying at about 35, 39.5 and 44 eV are due to excited states of  $\text{Mg}^+$  and Mg [3]. These are situated atop of a broad structure, which is attributable to bulk LVV emission, involving transitions from the valence band [1–6, 10]. As shown previously for the Mg [3] and Al [9] targets the electron spectrum from ion and neutral scattering are similar, in agreement with our charge fraction results.

The electron spectrum for scattering on the Na layer is shown in figure 1(a) and 2. Besides the peaks due to the auto-ionization of Ne states, the spectrum also displays a large peak at about 26 eV, which as in the case of Mg is situated on a large shoulder. The peak is attributed to decay of excited sputtered Na atoms in the  $2p^53s^2$  state. We attribute the shoulder to bulk Na emission as for the Mg case. Indeed this structure has a characteristic dependence on the observation angle with respect to the surface plane, as observed also for Mg, i.e. it is most prominent for observation angles close to the normal to the surface. The determination of the workfunction  $\phi$ , based on the observation of the shift of the  $\text{Ne}^{**}$  lines relative to other surfaces, yielded a value of about 2.65 eV, i.e. of the order of bulk Na  $\phi$  values existing in the literature. This allows us to conclude that in our experiment prolonged evaporation did produce a bulklike Na film. The peaks observed in the spectra are thus attributable to collisions on Na atoms only.

The results of measurements of electron emission for incident  $\text{He}^+$  are summarized in figure 1(b) for the Na, Mg and Al targets. The spectrum for scattering on Na displays a peak due decay of excited sputtered Na atoms in the  $2p^53s^2$  state and a peak lying at higher energies which is due to auto-ionization of the  $\text{He}^{**} 2s^2$  state, with a nominal energy of 33.2 eV (figure 1(b) iii). Electron energy spectra for He scattering on Mg (figure 1(b) ii) and Al (figure 1(b) i) also show excitation of this He state. We were not able to observe its production for scattering on Si. We did not perform charge fraction measurements for

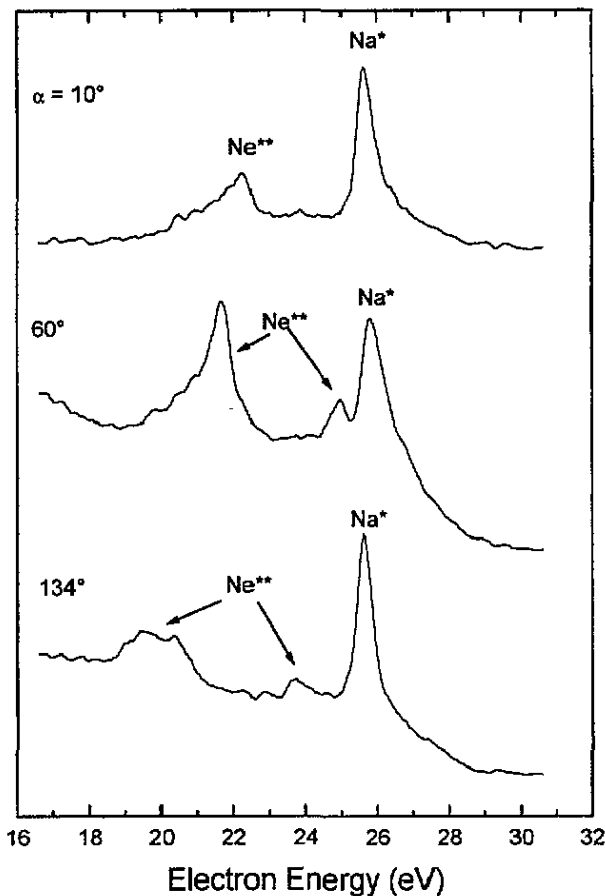


Figure 2. Energy spectra of electrons produced in 2 keV  $\text{Ne}^+$  incident at  $6^\circ$  on a Na surface for various observation angles.

$\text{He}/\text{He}^+$  scattering, but previous studies [23] have shown the production of ions in binary collisions involving these targets.

In the case of  $\text{Ar}^+$  scattering, we did not observe  $\text{Ar}^{**}$  state production. The electron energy spectra display peaks due to target excitation [1, 9, 10] only.

Thus we find that in all the cases considered, in so far as the projectile is concerned, excitation involves the lighter, smaller- $Z$  partner and thus follows the same pattern as in gas-phase collisions. Indeed existing experimental data [17–22] for  $\text{Na}^+$ ,  $\text{Mg}^+$  and  $\text{Al}^+$  scattering on He, Ne and Ar and  $\text{He}^+$  scattering on Na vapours shows that He and Ne are excited, while Ar excitation is extremely weak. Note that in all cases excitation of the target metal ion/atom was observed. Gas-phase data for Si were not found.

This first analogy established, it was interesting to study the energy dependence of excited-state production and in particular compare data in gas-phase and ion–solid collisions. The intensities of the main auto-ionization peaks were determined as a function of incident energy for  $6^\circ$ ,  $15^\circ$  and  $30^\circ$  incidence angles. These are shown for the Mg target (figure 3). These intensities correspond to integrals of peak areas after background subtraction and normalizing to the incident ion beam current. It is generally found that the peaks have the highest intensity for the highest grazing angle. Though accurate comparisons between

measurements for different angles are difficult, due to variations in the size of the incident beam on the sample and the unknown effective volume seen by the analyser optics, this result seems reasonable, because the reflection coefficient for Ne should decrease for larger incidence angles. Indeed, Ne scattering simulations on Mg, using the Marlowe code [24], show that for a 2 keV incident energy the reflection coefficient, defined as the number of backscattered to the number of incident particles, is 0.82, 0.3 and 0.09 for  $6^\circ$ ,  $15^\circ$  and  $30^\circ$  incidence angles respectively.

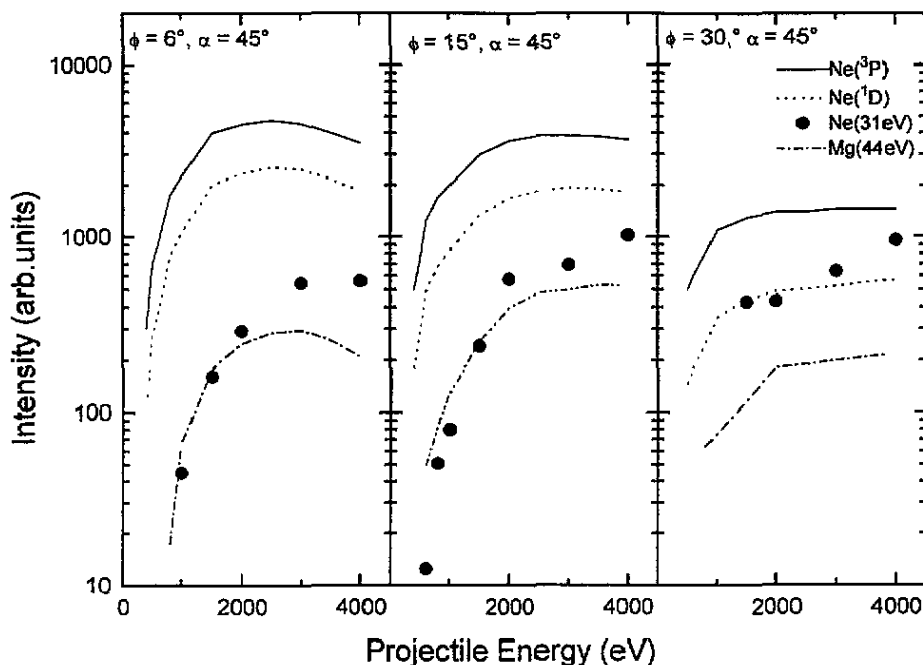


Figure 3. Energy dependence of auto-ionising-state production of Ne scattering on Mg for various incidence angles ( $\phi$ ) and a detection angle of  $\alpha = 45^\circ$ .

The general trends apparent from our measurements are that

(i) the efficiency of auto-ionizing-state production generally increases with collision energy in the range of energies below 3 keV (the Na case is an exception),

(ii) the ratio of the intensities of peaks due to  $^3P\ 3s^2$  and  $^1D3\ s^2$  states *decreases with increasing collision energy*, and

(iii) the ratio of the intensity of the peak due to the  $^1D3s^2$  state to that due to the  $^3P3s^2$  state decreases as the incident angle increases.

The latter effect is more clearly illustrated in figure 4. As will be further discussed below, this indicates that the production of these states is not determined solely by the binary collision, but that there exist other, surface-induced, core rearrangement processes [25, 26].

Figure 5 shows a comparative plot of the intensities summed over the Ne  $^3P3s^2$  and the  $^1D3s^2$  states for the different targets for a  $15^\circ$  incidence angle. As may be seen, in the studied energy range, the intensity increases as we go from the Si to the Na target. This

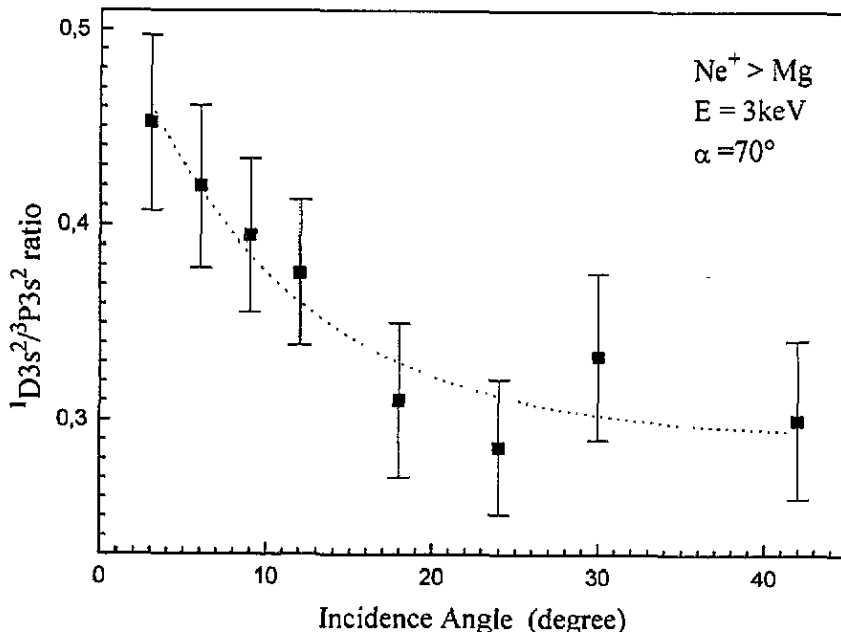
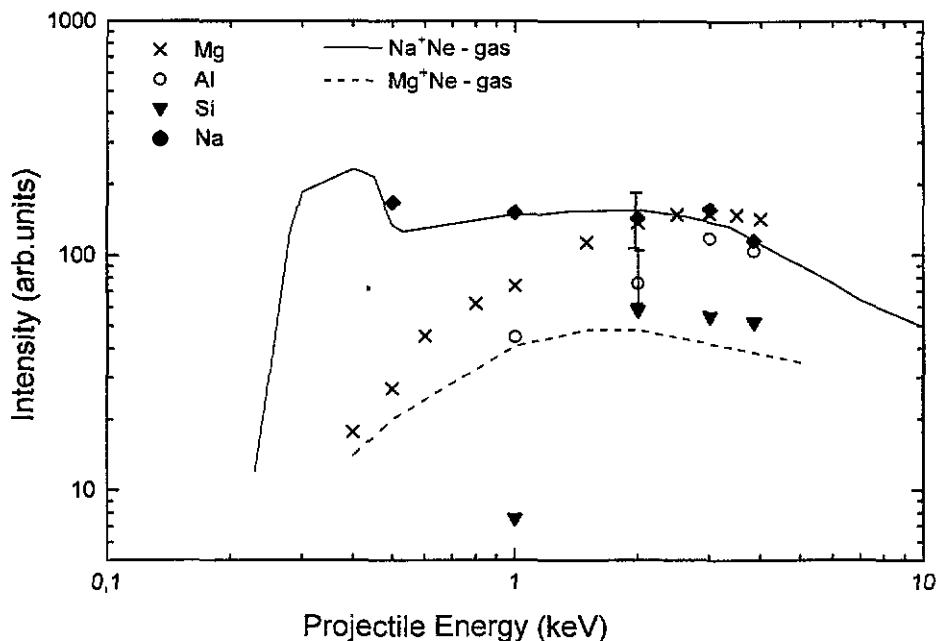


Figure 4. Incident angle dependence of the intensity of auto-ionizing peaks for  $\text{Ne}^+/\text{Mg}$  collisions.

trend in the excited-state production was also observed in measurements of ion fractions, as mentioned above.

These results are similar to what is observed in gas-phase atomic collisions. Figure 5 also shows the cross-section of summed  $\text{Ne}^{**}$  excited-state production measured for gas-phase collisions of  $\text{Na}^+$  [17] and  $\text{Mg}^+$  [19] with Ne. As may be seen in gas-phase collisions in case of the Na projectile, excitation processes are important at low energies. This is also the case for the Na solid target. In the case of Mg both in the gas phase and for the solid target excitation processes become important at higher energies. Note that the reflection coefficients at e.g. 500 eV for amorphous Na, Mg, Al and Si as estimated from Marlowe simulations are 0.63, 0.5, 0.75 and 0.6 respectively and are therefore not responsible for the very large differences in excited-state production at low energies. Direct comparison of these gas-phase and solid data is difficult, because the data for the solid represent only the  $3s^2$  state. In gas phase collisions of Na, Mg and Al ions, one observes a substantial amount of higher-lying auto-ionizing states [17–20], a difference to which we shall return below.

The similar general trends suggest that, both in gas-phase collisions and in ion-surface scattering, similar *primary excitation mechanisms* [13, 17] are operative. In gas-phase atom-atom collisions these are discussed in terms of the molecular orbital promotion model [13, 17–22]. Excitation processes, in e.g. all the cases considered here for Ne, involve the promotion of the  $4f\sigma$  orbital, which is correlated to the outermost  $2p$  orbital of Ne. Excited state production results from one or two electron transitions from the  $[\dots 3d\pi^4 4f\sigma^2 \dots]$  core molecular states. This explains the *strong excitation of e.g.  $\text{Ne}^{**}$*  [9–11, 17–20]. Note that experimental and theoretical studies in gas-phase collisions of Na, Mg and Al scattering on Ne indicate that the internuclear distances at which the  $4f\sigma$  promotion occurs are of the order of 1.45 atomic units ( $a_0$ ) [17],  $1.2a_0$  [18, 19] and  $0.85a_0$  [20] respectively. From a naive, qualitative, purely geometric point of view, this indicates that the excitation cross-



**Figure 5.** Efficiency of auto-ionizing-state production in  $\text{Ne}^+$  scattering on Na, Mg, Al and Si surfaces. The lines represent the total cross-section for  $\text{Ne}^{2+}$  auto-ionizing-state production in  $\text{Na}^+$  and  $\text{Mg}^+$  collisions [17] with a Ne target.

section will decrease as we go from Na to Al. This also corresponds to our observations for the solid target and the Si data follow this trend.

The similarities observed between the gas-phase and solid target data strongly suggest that the same primary excitation mechanism is involved i.e. the ionization and excitation processes of Ne observed are also due to one and two electron transitions from the  $4f\sigma$  MO following its promotion. In case of He they involve the  $3d\sigma$  MO promotion [10, 21, 22]. There do exist intriguing differences in the nature of excited-states produced in gas-phase and in collisions with surfaces. Thus in the Ne/Ne<sup>+</sup> surface collisions one observes

(i) the dominance of the  $^3\text{P}3s^2$  state, whereas states of the  $^3\text{P}$  core are only weakly excited in gas-phase collisions, in agreement with what is expected in the MO description for dissociation of the  $3d\pi^4$  core into only the  $^1\text{D}/^1\text{S}$  core atomic states and

(ii) the very weak-excitation of higher-lying states such as the  $3s3p$  and  $3p^2$  ones.

The nature of the excited-states formed in the surface collision involving valence orbitals is not clear, since it is not clear how one should consider transitions from the promoted orbital to higher-lying orbitals. However, it should be remembered here that the scattered particle starts from 'inside' the surface, at distances of the order of an atomic unit from surface atoms. Therefore, because of image-potential-induced level shifts in most cases considered, excitation will actually lead to ionization near the surface. One-electron excitation will lead to e.g.  $\text{Ne}^+$  production, while two-electron excitation processes lead in particular in the production of  $\text{Ne}^{2+}(^1\text{D})$  near the surface [14–16, 25, 26]. This turns out to be equivalent to considering, as in a model proposed by Joyes [27], that for a collision involving a solid the  $4f\sigma$  orbital is promoted above the Fermi level limit and this promotion then leads to one- or two-electron loss. The formation of excited particles and



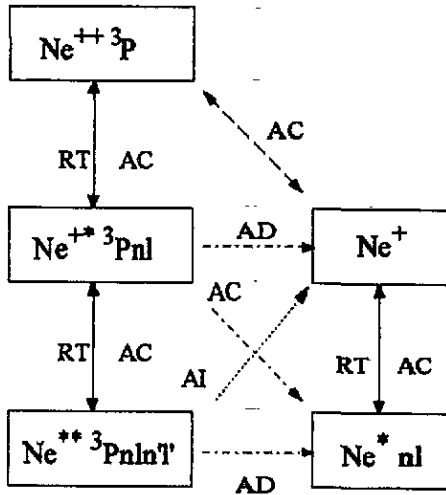


Figure 6. Electron loss and capture scheme between various  $Ne^{++}$ ,  $Ne^+$ ,  $Ne^*$  states for the  $3P$   $Ne^{++}$  core. The various Auger capture (AC), Auger de-excitation (AD), resonant transfers (RT), auto-ionization (AI) channels between states are indicated.

ions is then a result of a series of electron capture, loss and de-excitation processes which occur as the particles fly away from the surface [25,26]. This is schematized in figure 6 for one of the possible  $Ne^{2+}$  core states. Note that it seems reasonable to assume that the aspect of the gas-phase interpretation concerning the  $1D$  core production is conserved here, because we are dealing with an inner, unpromoted orbital. As discussed in [25,26], there exist several core rearrangement processes, which must account for the dominant  $3P$  core production observed experimentally. The above-noted difference, i.e. the very small magnitude of higher-lying  $Ne^{**}$  excited-states in case of solid targets, results from the fact that their binding energies are small and most of these lie above the Fermi level of the solid. Electron capture population of these states will therefore not occur. States like the  $Ne^{**} 3s3p/3p^2$  ones with intermediate binding energies of the order of 4 eV can only be formed in some cases and then only at large ion-surface distances. Their population will then be small, as may be seen from numerical simulations [26]. This explains the dominance of the more strongly bound (*circa* 7.2 eV)  $3s^2$  states.

We thus see that excited-state production in inelastic 'binary' collisions with surface atoms can be accounted for in terms of the gas-phase electron promotion model insofar as the primary excitation mechanism is concerned and reasonable conclusions concerning the particle that will be dominantly excited can be drawn from this description. The final excited-state distribution is however determined by surface-specific electron capture, loss, de-excitation and core rearrangement processes, which lead to a dominant selective production of the lower-lying excited-states. A final comment seems useful here. In spite of the fact that the general trend in excited-state production resembles the one observed in gas-phase collisions, trying to extract threshold values for excitation processes and critical molecular internuclear distances from ion-surface collision data does not seem to be a reliable procedure. This is because one should take into account particle reflection coefficients and because of the existence of the surface-induced processes. Thus one should consider that processes such as Auger de-excitation are favoured, the longer the particle spends near the surface, in other words at low energies. Hence the appearance threshold of e.g. the  $Ne^{**}$  states will not correspond to the 'actual' threshold for excitation.

## References

- [1] Valeri S 1993 *Surf. Sci. Rep.* **17** 85
- [2] Benazeth C, Benazeth N and Viel L 1978 *Surf. Sci.* **78** 625
- [3] Zampieri G, Meier F and Baragiola R 1984 *Phys. Rev. A* **29** 116
- [4] Gallon T E and Nixon A P 1992 *J. Phys.: Condens. Matter* **4** 9761
- [5] Pepper S V and Aron P R 1986 *Surf. Sci.* **169** 14
- [6] Grizzi O, Shi M, Bu H, Rabalais J W and Baragiola R A 1990 *Phys. Rev. B* **41** 4789
- [7] Rabalais J W, Chen J N and Kumar R 1985 *Phys. Rev. Lett.* **55** 1124
- [8] Souda R and Aono M 1986 *Nucl. Instrum. Methods B* **15** 114
- [9] Esaulov V A, Guillemot L and Lacombe S 1993 *Nucl. Instrum. Methods Phys. Res. B* **90** 305
- [10] Lacombe S, Guillemot L, Huels M, Vu Ngoc T and Esaulov V A 1993 *Surf. Sci.* **295** L1011
- [11] Lacombe S, Guillemot L, Huels M, Vu Ngoc T and Esaulov V A 1993 *Surf. Sci. Lett.* **295** L1011
- [12] Xu F, Mandarino N, Oliva A, Bonanno A, Zoccoli P, Camarca M and Baragiola R 1995 *Phys. Rev.* submitted
- [13] Barat M and Lichten W 1972 *Phys. Rev. A* **6** 211
- [14] Guillemot L, Lacombe S, Esaulov V, Maazouz M, Mandarino N, Sanchez E, Drobnich V, Bandurin Yu and Daschenko A I 1995 *Surf. Sci.* in preparation
- [15] Lacombe S, Esaulov V, Guillemot L, Maazouz M, Mandarino N and Sanchez E 1995 *Surf. Sci.* in preparation
- [16] Lacombe S, Esaulov V, Guillemot L, Maazouz M and Sanchez E 1995 in preparation
- [17] Ostgaard Olsen J *et al* 1979 *Phys. Rev. A* **19** 1457
- [18] Fayeton J, Anderson N and Barat M 1976 *J. Phys. B: At. Mol. Phys.* **9** L149
- [19] Fayeton J 1976 *Thesis* Université de Paris Sud, Orsay, France
- [20] Doweck D 1978 *Thesis* Université de Paris Sud, Orsay, France
- [21] Vu Ngoc T and Pommier J 1980 *8ème Colloque sur la Physique des Collisions Atomiques et Moléculaires (Lovain-la-Neuve)*
- [22] Courbin-Gaussorgues C, Vaaben V and Sidis V 1983 *J. Phys. B: At. Mol. Phys.* **16** 2817
- [23] Souda R and Aono M 1986 *Nucl. Instrum. Methods B* **15** 114
- [24] Robinson M T and Torrens I M 1974 *Phys. Rev. B* **9** 5008
- [25] Esaulov V, Guillemot L, Lacombe S and Vu Ngoc T 1995 *Nucl. Instrum. Methods Phys. Res. B* at press
- [26] Esaulov V 1994 *J. Phys.: Condens. Matter* **6** L699
- [27] Joyes P 1969 *J. Physique* **30** 243